Desalination and Water Treatment
www.deswater.com

doi: 10.5004/dwt.2020.26263

204 (2020) 400–412
November

Solvothermally synthesized spherical copper hydroxyfluoride (CuOHF) as an efficient heterogeneous Fenton catalyst for degrading organic pollutants

Zhiyang Yao, Tao Gu, Tianliang Lu, Yuzhong Zhan*

School of Chemical Engineering, Zhengzhou University, Zhengzhou 450001, China, Tel./Fax: +86-0371-67783051; emails: zhanyz@zzu.edu.cn (Y. Zhan), 810504475@qq.com (Z. Yao), 1904079632@qq.com (T. Gu), lutianliang@zzu.edu.cn (T. Lu)

Received 6 February 2020; Accepted 12 June 2020

ABSTRACT

Using $Cu(NO_3)_2{\cdot}3H_2O$ and NH_4NO_3 as raw materials, a series of copper hydroxyfluoride (CuOHF) catalysts were synthesized with various amounts of HF addition by the solvothermal method at 110°C. The products were characterized by X-ray diffraction, Fourier transform infrared, scanning electron microscopy. Their catalytic activity as heterogeneous Fenton catalysts was evaluated by using rhodamine B (RhB) as a simulated pollutant. The results showed that the amount of HF addition significantly affected the catalytic activity of the products. Their activity depended on not only the chemical composition but also the physical structure of the products. The spherical CuOHF synthesized under the condition of F/Cu = 1.7 showed the highest catalytic activity. The hierarchical structure of the spherical CuOHF may enhance the catalytic activity by providing more active sites. Using this CuOHF as the catalyst, the decolorization efficiency of 98% were reached for 50 mg/L RhB in 120 min under the condition of 40°C, pH 4.5, 20 mmol/L H_2O_2, and 0.15 g/L CuOHF. Under the same condition, the removal of TOC reached near 50%. This CuOHF also showed a wide usable pH range (3.5–9.5), high H_2O_2 utilization, and excellent stability. The highly oxidized $HO^{\bullet}$ generated by the spherical CuOHF activating H_2O_2 contributed to the degradation of the pollutant.

Keywords: Copper hydroxyfluoride; Solvothermal synthesis; Heterogeneous Fenton; Advanced oxidation

1. Introduction

Wastewaters discharged by many industries contain toxic organic substances such as dyes, drugs, pesticides, and phenols. These pollutants are difficult to be treated by conventional biological systems, seriously threatening the water ecological environment. Treating these pollutants by physical methods, such as flocculation, adsorption, and membrane technique can only separate pollutants, which still need to be further treated [1]. Chemical methods, especially advanced oxidation processes (AOPs), can degrade these recalcitrant organic pollutants into harmless small molecules such as water and carbon dioxide by highly active free radicals [2–5]. An example of AOPs is the classical Fenton method. In this method, Fe^{2+} ions are employed to activate H_2O_2 generating hydroxyl radicals ($^{\bullet}OH$), the second strongest oxidant known after fluorine. The classical Fenton method has been widely used in commercial treatment systems because of its high activity and mild operating conditions [6,7]. However, some obvious defects, such as a narrow acidic pH range (2.5–3) of operation, the low utilization efficiency of H_2O_2, and a large residue of iron hydroxide, hamper the wider application of this method. To overcome these defects, heterogeneous Fenton catalysis with solid Fe-containing materials instead of homogeneous Fe^{2+} ions has been widely concerned [8–11]. Nevertheless,

* Corresponding author.

when using these Fe-containing materials as heterogeneous Fenton catalysts, their highest catalytic activity appeared usually still at weak acid conditions of around pH 3 [6,12–15]. In view of this, much attention has been paid to non-iron materials in recent years [16]. Copper may be the most studied active species of non-iron heterogeneous Fenton catalysts, and Cu-containing materials usually have a wider pH range of application [16,17]. Studied Cu-containing active materials include copper oxide, cuprous oxide, layered hydroxy copper salt, etc. [16–26]. Low activity and poor stability of the catalysts were the main obstacles to practical application. Therefore, exploring new catalytic materials is still an important work.

Copper hydroxyfluoride (CuOHF, CAS 13867-72-6), also known as cupric hydroxide fluoride, copper hydroxide fluoride, or copper fluoride hydroxide, is a layered hydroxyl salt (LHS) with brucite structure [27]. The layer structure is formed by sharing edges of $Cu(OH)_3F_3$ octahedrons. In an octahedron, one F atom and three O atoms connect with one Cu atom on the equatorial plane, and the other two F atoms are located at the two ends of the octahedron, which connect with the Cu atom through the elongated F–Cu bonds. O atoms is further bound to H atoms forming hydroxyl groups (–O–H). These layers are connected to each other by hydrogen bonds (–O–H ····· F).

CuOHF is mainly used as a sensitizer in the atomic emission spectrometric analysis, which can significantly improve the determination sensitivity of boron and silicon [28]. There are few studies on its synthesis and application. The only example as a catalyst was reported by a Chinese patent (CN 103274917A) that CuOHF catalyzed the synthesis of benzoyl derivatives from diphenylacetylene. In this reaction, the CuOHF catalyst was prepared complicatedly by mixing the copper powder with 1-Chloromethyl-4-fluoro-1,4-diazabicyclo [2,2,2] octane bis (tetrafluoroborate) in the mixed solvent of organic solvent and water.

In this study, we report the solvothermal synthesis of CuOHF and its catalytic performance as a heterogeneous Fenton catalyst for the first time. We found that the structure and morphology of the synthesized products obviously affected the catalytic performance. The spherical CuOHF showed high catalytic activity, good stability, and effective H_2O_2 utilization.

2. Methodology

2.1. Preparation of catalysts

The catalysts were synthesized by a solvothermal method using anhydrous ethanol as solvent. In a Teflon-lined stainless steel autoclave, 0.97 g of copper nitrate ($Cu(NO_3)_2{\cdot}3H_2O$) and 0.16 g of ammonium nitrate (NH_4NO_3) were mixed in 30 mL of anhydrous ethanol. Then a certain amount of hydrofluoric acid (HF, 40%) was dropped in the ethanol solution under stirring. The autoclave was sealed and put into an oven. The crystallization was carried out at 110°C for 20 h without stirring. The autoclave was then quenched to room temperature and the solid product was filtered, washed, and dried at 80°C for 8 h. To investigate the effect of HF amount on the synthesis, various amount of HF was added and the range of F/Cu ratio was 0–3.4.

2.2. Characterization of catalysts

X-ray diffraction (XRD) patterns of the synthesized products were determined by using a D8 advance X-ray diffractometer (Bruker, German) employing Cu K_α radiation. Fourier transform infrared (FTIR) spectra were obtained on a WQF-510 FTIR spectrophotometer (BRAIC Co., China). Scanning electron microscopy (SEM) images were recorded on a JSM-7500F SEM (JEOL, Japan). X-ray photoelectron spectroscopy (XPS) measurements were conducted on a Thermo Scientific-Escalb 250XI electron spectrometer (Thermo Scientific Inc., USA).

2.3. Evaluation of catalytic activity

The catalytic activity of the synthesized products as heterogeneous Fenton catalysts was evaluated using rhodamine B (RhB) as a simulated pollutant. The degradation experiments of RhB were carried out in a glass reactor of 400 mL with magnetic stirring. The reactor was immersed in a constant temperature water bath. In a typical run, 200 mL of RhB solution (pH = 4.5) with the concentration of 50 mg/L and 30 mg of the synthesized catalyst were added in the reactor (catalyst dosage 0.15 g/L). After the temperature was constant at 40°C, the degradation was initiated by adding 4 mL of H_2O_2 solution, which was diluted by 10-fold with hydrogen peroxide reagent (H_2O_2, 30%) before the experiment. In this case, the H_2O_2 dosage was 20 mmol/L. At given time intervals, a 5 mL solution was taken out and centrifuged immediately to remove the residual catalyst. The solution concentration of the dye was measured at the maximum absorption wavelength (554 nm) of RhB using a UV-2450 UV-vis spectrophotometer (Shimadzu, Japan). The decolorization efficiency (η) of RhB solution was calculated by the following equation:

$$\eta = \frac{C_0 - C_t}{C_0} \times 100\% \quad (1)$$

where C_0 is the initial concentration of RhB, and C_t is the concentration of RhB at time t.

To study the effect of variables on the degradation, the experiments were repeated under different initial pH values (3.5–9.5), catalyst dosages (0–0.5 g/L), H_2O_2 dosages (0–50 mmol/L), initial dye concentrations (25–150 mg/L), and temperatures (30°C–60°C). If necessary, the pH of the RhB solution was adjusted by adding a small amount of NaOH or H_2SO_4 solution. Unless otherwise specified, the operating parameters were the same as those of the typical run.

The UV-vis absorption spectra of RhB degradation process were also recorded using the UV-2450 UV-vis spectrophotometer. The removal of total organic carbon (TOC) was monitored using an Elab-TOC TOC analyzer (Suzhou Elab Analytical Instrument Co., Ltd., China).

3. Results and discussion

3.1. Preparation of CuOHF

3.1.1. XRD analysis

We have reported the solvothermal synthesis of copper hydroxynitrate ($Cu_2(OH)_3NO_3$) at a higher temperature

of 150°C by using $Cu(NO_3)_2{\cdot}3H_2O$ and NH_4NO_3 as raw materials. Due to the high temperature, a trace amount of Cu_2O formed by the reduction of Cu(II), doping in the $Cu_2(OH)_3NO_3$ phase [29]. In this study, the synthesis temperature was lowered to 110°C and the pure $Cu_2(OH)_3NO_3$ without Cu_2O impurity was obtained (Fig. 1a and Fig. S1). When adding a small amount of HF (F/Cu = 0.6) to this synthesis system, the $Cu_2(OH)_3NO_3$ diffraction peaks of the product decreased significantly, while the obvious CuOHF diffraction peaks appeared [30]. When increasing HF to F/Cu = 1.1, which is only slightly higher than the theoretical amount of CuOHF, the $Cu_2(OH)_3NO_3$ diffraction peaks disappeared completely, indicating the pure CuOHF product was synthesized. When further increasing the amount of HF, the intensity of 001 peak increased rapidly and the width of the peak narrowed obviously. Meanwhile, 12-1 peak shifted obviously, 120 and 12-2 peaks shifted slightly to the low angle, but 001 and 20-2 peaks almost remained constant (Fig. 1a and Fig. S2). These results showed that CuOHF was stabler in this solvothermal system, and $Cu_2(OH)_3NO_3$ was easy to be converted into CuOHF. This conversion was accomplished by partially replacing O atoms of $Cu(OH)_6$ octahedrons with F atoms to form $Cu(OH)_3F_3$ octahedrons. When the addition of HF was low, F content of CuOHF did not achieve the theoretical amount, thus a small amount of $Cu(OH)_4F_2$, $Cu(OH)_5F_1$, or $Cu(OH)_6$ octahedrons still existed in the structure of CuOHF. This inconsistency of structural units resulted in the lower crystallinity of the synthesized products. With the increase of HF, more $Cu(OH)_3F_3$ octahedrons formed and the crystallinity of CuOHF increased. The elongated F–Cu bonds at the two ends of the octahedrons may form finally, mainly resulting in elongation in the *b* direction of the crystal cell of CuOHF. So, the layer spacing (d_{001}) almost kept constant and the 12-1 peak obviously shift to the low angle (Fig. S1).

It should be pointed out that if NH_4F was used instead of HF, the pure phase of CuOHF cannot be synthesized, and the product was mainly $Cu_2(OH)_3NO_3$ mixed with a small amount of CuOHF. When using HNO_3 instead of HF, the formation of $Cu_2(OH)_3NO_3$ was not affected (Fig. 1b). These results showed that the acidity of HF played an important role in the formation of CuOHF pure phase.

3.1.2. FTIR analysis

The influence of the amount of HF on the synthesis was further confirmed by FTIR (Fig. 2). Without adding HF, the FTIR spectrum of the product was consistent with that of $Cu_2(OH)_3NO_3$ reported in the literature [31,32]. The absorption peak between 3,600 and 3,000 cm^{-1} was caused by the stretching vibration of O–H, and the peak near 3,544 cm^{-1} indicated the existence of free O–H groups. The peaks at 1,422 and 1,337 cm^{-1} belonged to the antisymmetric and symmetric stretching vibration of $–NO_2$, respectively. The peak at 1,047 cm^{-1} belonged to the stretching vibration of N–O bonds in $O–NO_2$ groups. The peak at 1,384 cm^{-1} indicated the existence of free NO_3^-. The absorption peaks at 878, 784, and 675 cm^{-1} are caused by the bending vibration of Cu–O–H. The different frequencies were due to the different degree of hydrogen bonding. The peaks at 512 and 427 cm^{-1} were attributed to the vibration of Cu–O. In particular, there was no characteristic absorption peak of Cu_2O in the range of 640–610 cm^{-1} [33,34], which further proved that $Cu_2(OH)_3NO_3$ synthesized at a lower temperature (110°C) did not contain Cu_2O impurity.

When a small amount of HF was added to the synthesis system (F/Cu = 0.6), the absorption peaks associated with $Cu_2(OH)_3NO_3$ decreased obviously, and some new absorption peaks began to appear. When HF was increased to F/Cu = 1.1, only a weak peak (1,384 cm^{-1}) of free NO_3^- remained. This result indicated that there existed residual NO_3^- in the synthesized CuOHF, although according to the XRD results the product should be pure CuOHF. With the increase of HF, the peak of free NO_3^- disappeared completely. In this case, the FTIR spectrum of pure CuOHF was obtained.

There are few studies on the vibration spectra of CuOHF. As far as we know, the infrared spectrum of CuOHF has not been reported, and its Raman spectrum was reported in only one paper [27]. Based on the Raman spectrum of CuOHF and the infrared absorption of related groups, we tried to assign the characteristic absorption peaks of CuOHF. The wide peak between 3,600 and 3,000 cm^{-1} was undoubtedly considered as the stretching vibration of O–H. The maximum absorption shifted to 3,176 cm^{-1} due to the formation of stronger hydrogen bond (–O–H ····· F). There was no

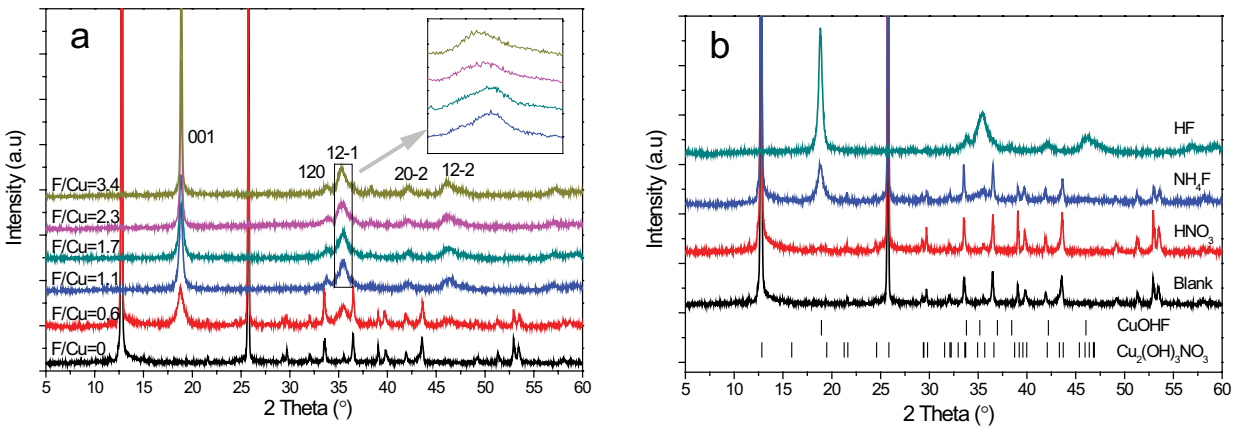

Fig. 1. XRD patterns of the products synthesized under (a) various amount of HF and (b) different additives.

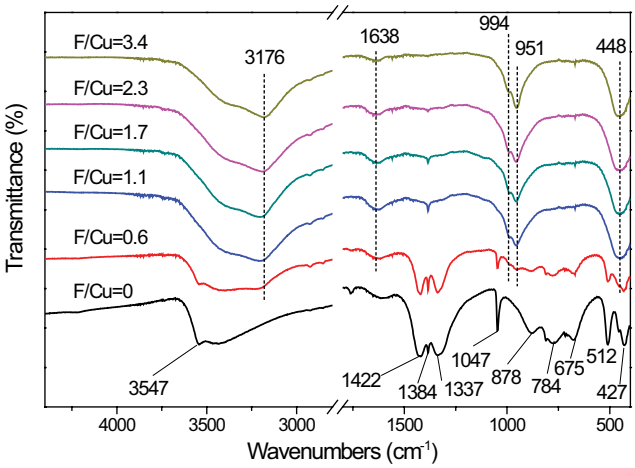

Fig. 2. FTIR spectra of the products synthesized under various amount of HF.

stretching vibration peak of the free O–H near 3,600 cm^{-1}. The absorption peak at 1,638 cm^{-1} belonged to the bending vibration of adsorbed water. The strong absorption peak at 951 cm^{-1} and the shoulder peak at 994 cm^{-1} can be attributed to the O–H deformation vibration. The peak at 448 cm^{-1} can be attributed to the vibration of Cu polyhedron.

3.1.3. SEM and XPS analysis

The SEM images of the samples synthesized under different amounts of HF are shown in Fig. 3. It can be seen from the figure that the morphology of $Cu_2(OH)_3NO_3$ synthesized without HF was mainly plate-like crystal. When a small amount of HF was added to F/Cu = 0.6, the sample was a mixture of plate-like crystal, small debris, and microsphere with a rough surface. Based on the XRD and FTIR analysis, it can be inferred that the small debris and microsphere was CuOHF. With the increase of HF content, the microsphere in the product increased gradually. When the F/Cu was up to 1.7, the product was almost microsphere with a diameter of about 5–15 μm. The microsphere had an intertexture-like hierarchical structure formed by thin sheets. However, with the further increase of HF addition, the regular microsphere decreased, and the disk-like product with a diameter of about 20 μm appeared.

The spherical product of F/Cu = 1.7 was further characterized by XPS, the results as shown in Fig. S3. The element composition (Cu_{2p} 935.5 eV, O_{1s} 532.0, and F_{1s} 684.4 eV) of the product was confirmed by the survey scan. The weak C1s peak at about 285 eV comes from carbon contaminants. The high-resolution spectrum of Cu_{2p} showed that there was Cu(II) in the product, because of the existence of shake-up peaks along with the main peaks [35].

3.2. Effect of synthesis conditions on catalytic activity

The catalytic activity of the products was significantly affected by the amount of adding HF in the synthesis system (Fig. 4). The pure $Cu_2(OH)_3NO_3$ synthesized without HF showed relatively low catalytic activity, and the decolorization efficiency of RhB was only about 30% in 20 min. With the increase of HF the catalytic activity of the products obviously improved. The microsphere of CuOHF synthesized at F/Cu = 1.7 exhibited the highest catalytic activity. The decolorization efficiency of RhB was up to about 70% in 20 min. The calculated initial first-order kinetic constant is 3.3 times higher than that of $Cu_2(OH)_3NO_3$. However,

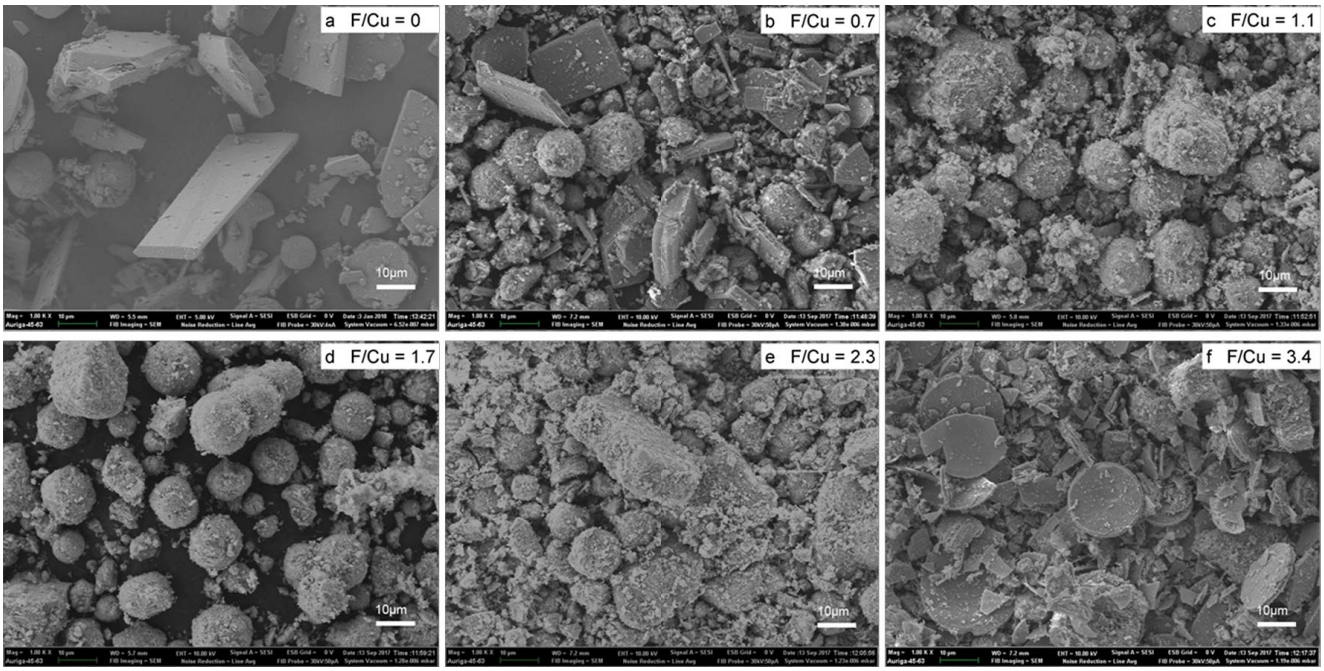

Fig. 3. SEM images of the products synthesized under various amount of HF.

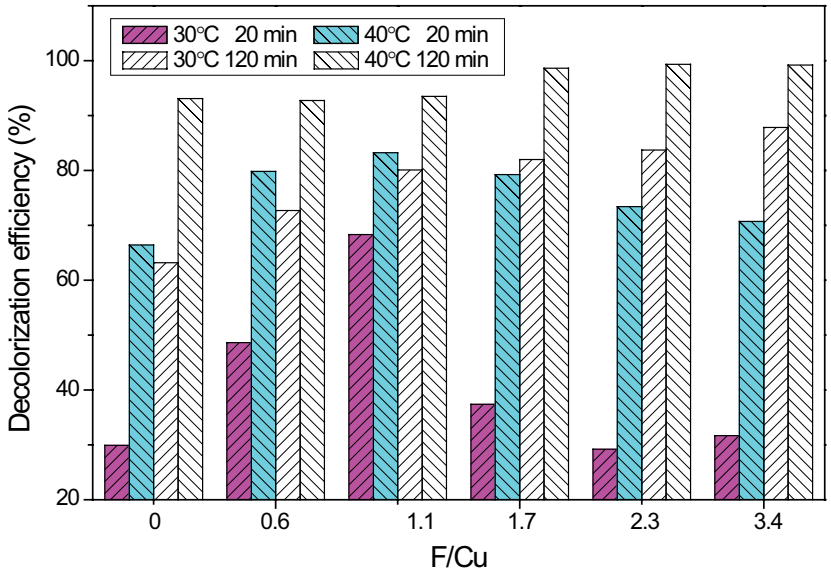

Fig. 4. Comparison of catalytic activity of the products synthesized under various amount of HF. The operating parameters were the same as those of the typical run described in the experimental section, except the catalysts dosage of 0.25 g/L.

the further increase of HF addition resulted in a decrease of catalytic activity. This indicated that the catalytic activity of the synthesized products depended on not only the chemical composition but also the physical structure. The hierarchical structure of the spherical CuOHF enhanced the catalytic activity by providing more active sites.

It should be noted that the catalytic degradation of the dye by the spherical CuOHF in 120 min was slightly lower than that by the other samples. This phenomenon may be the embodiment of high catalytic activity. Properly reducing the dosage of the catalyst can solve this problem (see the following discussion about the effect of the CuOHF dosage). If the degradation temperature increased from 30°C to 40°C, the catalytic activity of all samples enhanced significantly, and the difference in the activity between the samples decreased. In the following sections, the catalytic performance of only the spherical CuOHF was studied.

3.3. Effects of operation conditions on the dye degradation

3.3.1. Initial pH

The spherical CuOHF presented a wide range of usable initial pH (3.5–9.5) (Fig. 5a), which can reduce the operation cost of adjusting the pH before and after the wastewater treatment. At around the initial pH 4.5 the catalyst showed the highest catalytic performance. The decolorization efficiency reached about 80% in 20 min and 98% in 120 min. When pH increased to 9.5, the decolorization efficiency was still over 60% in 20 min and nearly 90% in 120 min.

3.3.2. CuOHF dosage

The effect of CuOHF dosage on the RhB degradation is shown in Fig. 5b. As a comparison, H_2O_2 itself showed very weak oxidative ability, and the decolorization efficiency was below 10% in 120 min. H_2O_2 can be activated significantly by adding only 0.05 g/L CuOHF as the catalyst. The decolorization efficiency was about 50% in 20 min and 98% in 120 min. This dosage was considerably lower than that of many heterogeneous Fenton catalysts reported in recent years [11], indicating CuOHF had high catalytic activity. Increasing CuOHF dosage can improve the initial degradation, but excessive catalyst (>0.15 g/L) reduced the final degradation instead. For example, when the CuOHF dosage was 0.5 g/L, the decolorization efficiency was about 80% in 20 min but only 87% in 120 min. This phenomenon was different from the decrease of degradation performance caused by excessive catalyst scavenging hydroxyl radicals, as reported in many literature [11]. It may be explained by the high catalytic activity of the spherical CuOHF for activating H_2O_2. The excessive catalyst contacted H_2O_2 with a relatively high concentration at the initial stage of the degradation, partially resulting in the decomposition of H_2O_2, because the hydroxyl radicals produced by catalytically activating H_2O_2 did not attack the dye immediately owing to the diffusion limitation. In fact, tiny bubbles were observed releasing from the surface of the catalyst at the initial stage of degradation. To reduce the H_2O_2 decomposition and improve its utilization, batch adding H_2O_2 should be a useful strategy.

3.3.3. H_2O_2 dosage

The efficient utilization of H_2O_2 plays a key role in reducing the cost of wastewater treatment when using Fenton process. However, the H_2O_2 dosage required in many heterogeneous Fenton processes was too high, usually dozens of times higher than the theoretical value [11]. The spherical CuOHF showed a high utilization of H_2O_2, as shown in Fig. 5c. According to the stoichiometric relationship, an H_2O_2 dosage of 7.3 mmol/L is theoretically required for completely mineralizing RhB of 50 mg/L (correspond to 0.1 mmol/L) [36]. When the H_2O_2 dosage was 5 mmol/L,

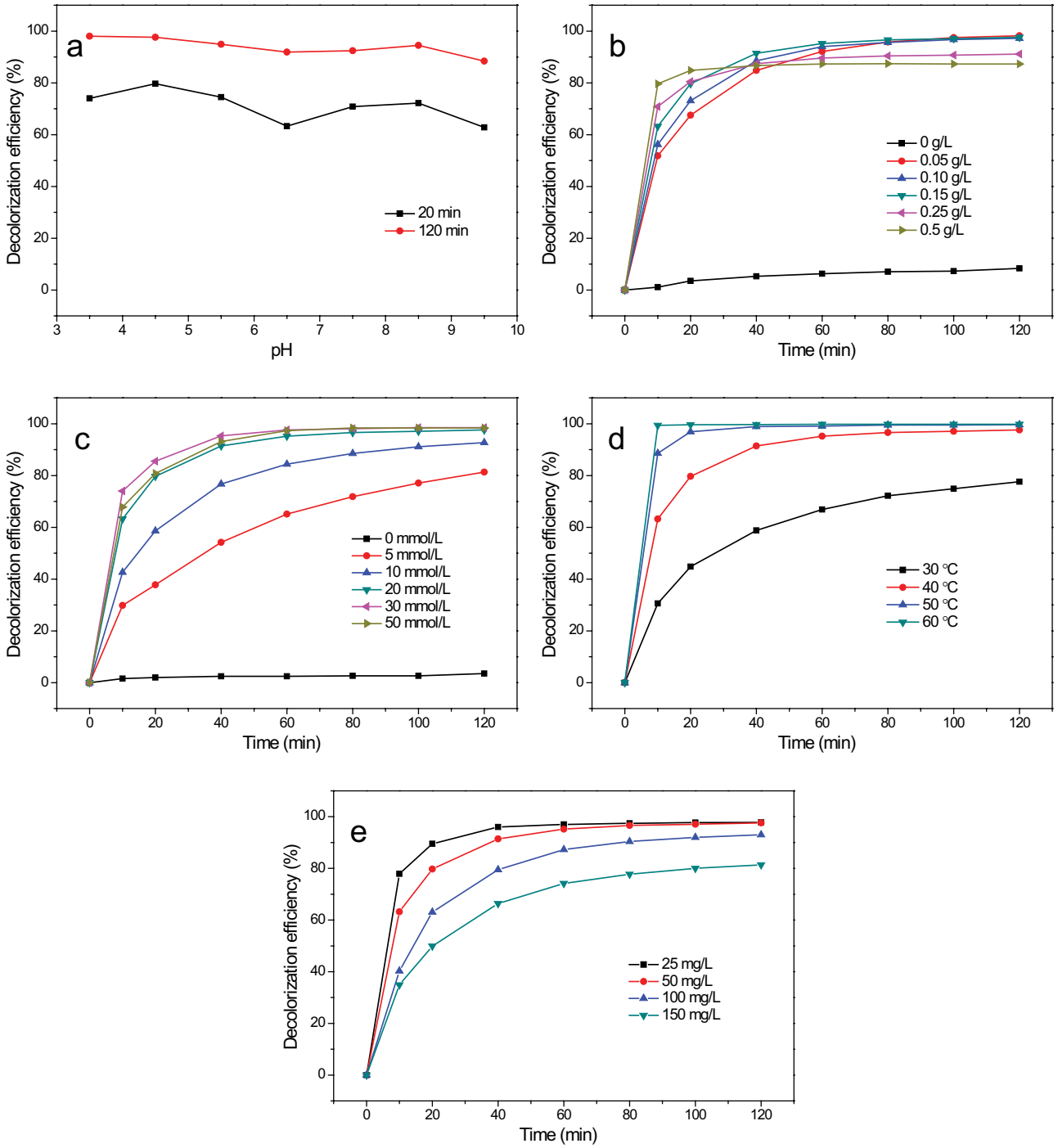

Fig. 5. Effect of operation parameters on the degradation of RhB. (a) initial pH, (b) CuOHF dosage, (c) H_2O_2 dosage, (d) degradation temperature, and (e) initial RhB concentration. The operating parameters are the same as the typical run described in the experimental section except the studied variable.

which is only 68% of the theoretical value, the decolorization efficiency was more than 80% in 120 min. When the H_2O_2 dosage was 10 mmol/L, which is only 1.4 times the theoretical value, the decolorization efficiency was about 93% in 120 min. When the dosage was 20 mmol/L, which is only 2.7 times the theoretical value, the decolorization efficiency reached about 98% in 120 min. Of course, decolorization of the dye does not mean its complete mineralization. Further increasing H_2O_2 dosage did not obviously improve degradation. An excessive H_2O_2 concentration would result in a decrease of the degradation, because H_2O_2 itself was a free radical scavenger [11]. On the other hand, almost no decoloration was observed in the absence of H_2O_2, indicating that the spherical CuOHF hardly adsorbed RhB.

3.3.4. Degradation temperature

Expectedly, increasing the temperature significantly increased the degradation, as shown in the Fig. 5d. The decolorization efficiency in 120 min was about 78% at 30°C and 98% at 40°C. When the temperature rose to 50°C and 60°C, the decolorization efficiency in 10 min was close to 90% and 100%, respectively. It can be expected that at a higher temperature, a better degradation can be achieved at a lower concentration of H_2O_2 and a smaller dosage of the catalyst.

3.3.5. Initial RhB concentration

The degradation at various initial concentration of RhB is shown in Fig. 5e. In these experiments, the initial H_2O_2 concentrations were kept at 20 mmol/L, so the decolorization efficiency of RhB decreased with the increase of initial RhB concentration. When the initial concentration of RhB was 100 mg/L, the decolorization efficiency reached more than 90% in 120 min, although in this case, the H_2O_2 dosage is only 1.4 times of the theoretical requirement. When the initial concentration of RhB was increased to 150 mg/L, the decolorization efficiency was still over 80%, in this case, the H_2O_2 dosage was only 91% of the theoretical value. These results also showed that the spherical CuOHF presented high activity and high utilization of hydrogen peroxide. It can be predicted that wastewaters with higher concentration can be more completely degraded by increasing temperature and H_2O_2 dosage.

3.4. Stability of the spherical CuOHF

The long-term stability of a catalyst is the key factor for its practical application. We tested the stability of the spherical CuOHF by filtering out the used catalyst, drying, and then reusing it to catalytically degrade RhB. The results showed that the spherical CuOHF had good stability. Although the third repeated experiment showed that the catalytic activity decreased slightly, and the decolorization efficiency in 120 min decreased from 98% in the first use to about 93%, the activity tended to be stable. In the fifth repeated experiment, the decolorization efficiency was still about 93% in 120 min (Fig. 6).

We also characterized the crystal phase, structure, and morphology of the spherical CuOHF before and after use by XRD, FTIR, and SEM (Figs. S4–S6). The results showed that the crystallinity of the used catalyst was lower than that of the fresh catalyst, but the crystal phase did not change and no new phase formed. The morphology remained spherical without obvious change.

3.5. Mechanism of catalytic degradation

The determination of effects of quenching agents on degradation is simple ways to identify active species [37,38]. The active species of Fenton process is HO•. In order to identify HO•, isopropanol as the HO• quenching agent was added into the reaction system, and the results are shown in Fig. 7. The addition of isopropanol almost completely inhibited the activity of the spherical CuOHF. In this case, the decolorization efficiency was only about 18% in 120 min. Nevertheless, without adding isopropanol, the decolorization efficiency was 98% in the same period. This result confirmed that HO• was produced by CuOHF activating H_2O_2 and acted as the dominating reactive species [38].

The UV-vis adsorption spectra of RhB degradation process are shown in Fig. 8. It can be seen that the RhB solution has a strong absorption peak at 554 nm attributed to xanthene-conjugated chromophore and an obvious absorption peak at 260 nm attributed to aromatic ring. The highly oxidized HO•, which was generated by the spherical CuOHF activating H_2O_2, destroyed the

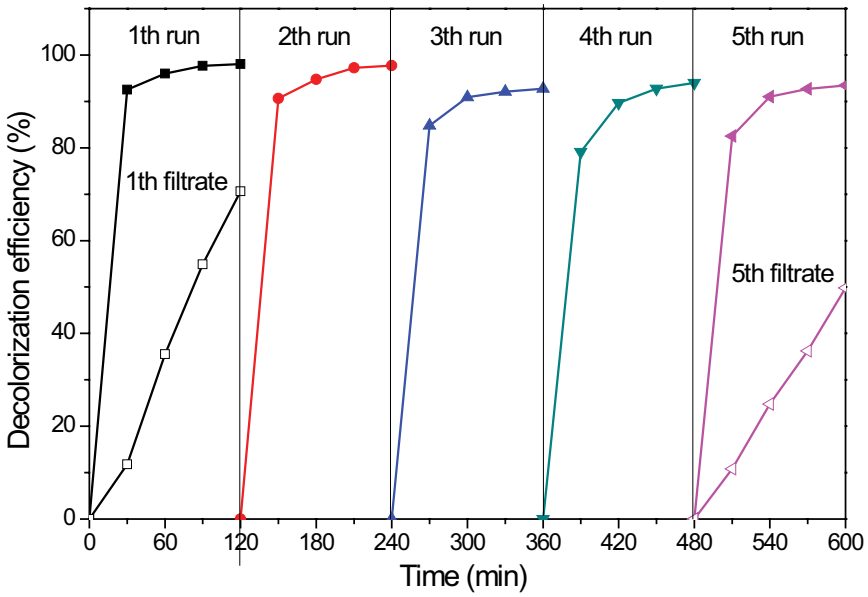

Fig. 6. Catalytic stability of the spherical CuOHF and the catalytic activity of the filtrate.

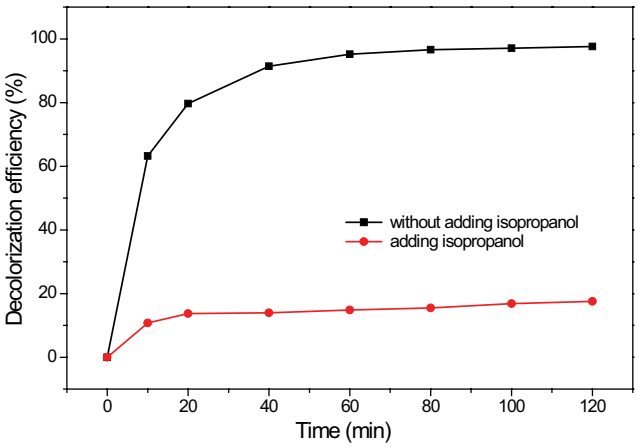

Fig. 7. Inhibition of adding isopropanol on the catalytic activity of the spherical CuOHF.

unsaturated bonds of these chromophores and conjugated groups rapidly, making these peaks drop sharply, and disappear almost at last [39,40]. As we all know, the oxidation decolorization of a dye does not mean its complete mineralization. We monitored the removal of TOC in the degradation process. The results showed that although the decolorization efficiency reached 98% in 120 min, the removal of TOC was only nearly 50%. This is mainly because the intermediate products such as formic acid and acetic acid are more difficult to be removed than dyes by Fenton oxidation. Although the dyes are not completely mineralized into inorganic substances, these intermediates are generally nontoxic, and easy to be further treated by conventional biological methods.

The leaching of metal species of heterogeneous Fenton catalysts is almost inevitable during the degradation processes [8]. Due to iron and copper ions is also used as homogeneous Fenton catalysts, in some cases, the degradation of pollutants may be mainly attributed to the homogeneous catalysis of leaching metal ions [41]. For the CuOHF catalyst not only Cu^{2+} but also F^- may leach out during the degradation process. There may be promoting effect of F^- on Cu-Fenton catalysis [36]. In order to confirm that the degradation is mainly attributed to the heterogeneous catalysis of the spherical CuOHF, we tested the homogeneous catalysis of the filtrate after dye degradation, and the results are also shown in Fig. 6. The results showed that the catalytic activity of the first filtrate was very low, and the decolorization efficiency was only about 30% in 30 min and 70% in 120 min, which were far lower than 93% in 30 min and 98% in 120 min when using CuOHF as the catalyst. This fully confirmed the degradation was mainly based on the heterogeneous catalytic activation of H_2O_2 by the CuOHF. After five repetitions the catalytic activity of the filtrate further lowered, and the decolorization efficiency decreased to only about 50% in 120 min. This also implied that after several repetitions the copper leaching decreased gradually and the CuOHF catalyst tended to be stable.

4. Conclusions

Copper hydroxyfluoride (CuOHF) was synthesized by a solvothermal method under various HF additions. Its catalytic activity as a novel heterogeneous Fenton catalyst was evaluated by using rhodamine B (RhB) as a simulated pollutant. The amount of HF addition significantly affected the catalytic activity of the products. The catalytic activity of the synthesized products depended on not only the chemical composition but also the physical structure. The spherical CuOHF synthesized under the condition of F/Cu = 1.7 showed the highest catalytic activity. The hierarchical structure of the spherical CuOHF may enhance the catalytic activity by providing more active sites. This CuOHF also showed a wide usable pH range and excellent stability. The highly oxidized HO•, which generated

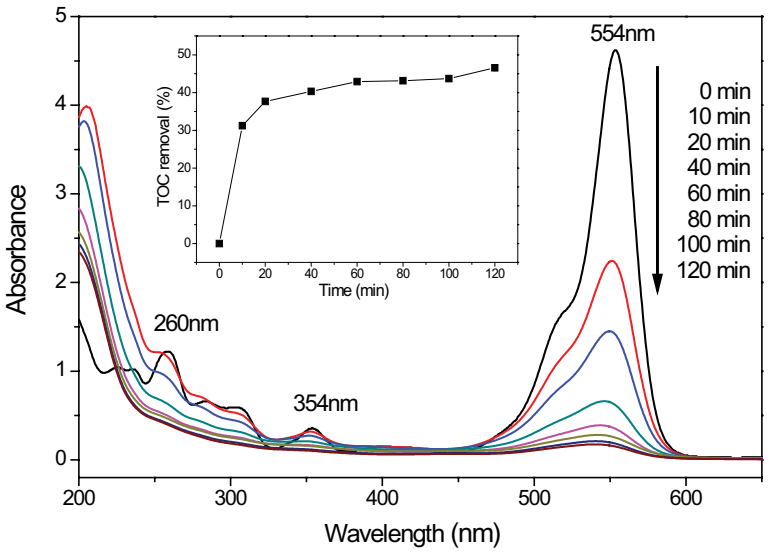

Fig. 8. UV-vis spectra of RhB during degradation process (insert: TOC changes with degradation).

by the spherical CuOHF activating H_2O_2, contributed to the degradation of the pollutant.

Acknowledgments

We are grateful to the National Natural Science Foundation of China (21802125) for financial supports.

References

[1] M.C. Collivignarelli, A. Abbà, M.C. Miino, S. Damiani, Treatments for color removal from wastewater: state of the art, J. Environ. Manage., 236 (2019) 727–745.
[2] D.S. Babu, V. Srivastava, P.V. Nidheesh, M.S. Kumar, Detoxification of water and wastewater by advanced oxidation processes, Sci. Total Environ., 696 (2019) 1–20, doi: 10.1016/j.scitotenv.2019.133961.
[3] R. Anjali, S. Shanthakumar, Insights on the current status of occurrence and removal of antibiotics in wastewater by advanced oxidation processes, J. Environ. Manage., 246 (2019) 51–62.
[4] C. Amor, L. Marchão, M.S. Lucas, J.A. Peres, Application of advanced oxidation processes for the treatment of recalcitrant agro-industrial wastewater: a review, Water, 11 (2019) 1–29, doi: 10.3390/w11020205.
[5] G. Lofrano, R. Pedrazzani, G. Libralato, M. Carotenuto, Advanced oxidation processes for antibiotics removal: a review, Curr. Org. Chem., 21 (2017) 1054–1067.
[6] C. Kantar, O. Oral, O. Urken, N.A. Oz, S. Keskin, Oxidative degradation of chlorophenolic compounds with pyrite-Fenton process, Environ. Pollut., 247 (2019) 349–361.
[7] A. Mirzaei, Z. Chen, F. Haghighat, L. Yerushalmi, Removal of pharmaceuticals from water by homo/heterogonous Fenton-type processes–a review, Chemosphere, 174 (2017) 665–688.
[8] P.V. Nidheesh, Heterogeneous Fenton catalysts for the abatement of organic pollutants from aqueous solution: a review, RSC Adv., 5 (2015) 40552–40577.
[9] L. Liu, S.S. Fan, Y. Li, Removal of methylene blue in aqueous solution by a Fenton-like catalyst prepared from municipal sewage sludge, Desal. Water Treat., 138 (2019) 326–334.
[10] Y. Zhu, R. Zhu, Y. Xi, J. Zhu, G. Zhu, H. He, Strategies for enhancing the heterogeneous Fenton catalytic reactivity: a review, Appl. Catal., B, 255 (2019) 1–16, doi: 10.1016/j.apcatb.2019.05.041.
[11] N. Wang, T. Zheng, G. Zhang, P. Wang, A review on Fenton-like processes for organic wastewater treatment, J. Environ. Chem. Eng., 4(2016) 762–787.
[12] N. Pandey, V. Kumar, P. Ghosh, Degradation of 4-nitrophenol (4-NP) using Fe-loaded fly ash brick clay as a heterogeneous Fenton catalyst, Desal. Water Treat., 95 (2017) 170–179.
[13] S.R. Pouran, A.A.A. Raman, W.M.A.W. Daud, Review on the application of modified iron oxides as heterogeneous catalysts in Fenton reactions, J. Cleaner Prod., 64 (2014) 24–35.
[14] Q. Ding, F.L.Y. Lam, X. Hu, Complete degradation of ciprofloxacin over g-C_3N_4-iron oxide composite via heterogeneous dark Fenton reaction, J. Environ. Manage., 244 (2019) 23–32.
[15] N. Inchaurrondo, A. Maestre, G. Žerjav, A. Pintar, C. Ramosc, P. Haure, Screening of catalytic activity of natural iron-bearing materials towards the catalytic wet peroxide oxidation of Orange II, J. Environ. Chem. Eng., 6 (2018) 2027–2040.
[16] A.D. Bokare, W. Choi, Review of iron-free Fenton-like systems for activating H_2O_2 in advanced oxidation processes, J. Hazard. Mater., 275 (2014) 121–135.
[17] M. Munoz, Z.M. De Pedro, J.A. Casas, J.J. Rodriguez, Preparation of magnetite-based catalysts and their application in heterogeneous Fenton oxidation–a review, Appl. Catal., B, 176 (2015) 249–265.
[18] Y. Fang, Y. Guo, Copper-based non-precious metal heterogeneous catalysts for environmental remediation, Chin. J. Catal., 39(2018) 566–582.
[19] J. Dong, H. Dong, L. Han, B. Fu, Y. Chen, Y. Zhan, Peroxide degradation of azo dye using hydrothermally synthesized Cu-L zeolite as high performance catalys, Desal. Water Treat., 56 (2015) 1056–1065.
[20] L. Zhang, D. Xu, C. Hu, Y. Shi, Framework Cu-doped $AlPO_4$ as an effective Fenton-like catalyst for bisphenol A degradation, Appl. Catal., B, 207 (2017) 9–16.
[21] Z. Su, J. Li, D. Zhang, P. Ye, H. Li, Y. Yan, Novel flexible Fenton-like catalyst: unique CuO nanowires arrays on copper mesh with high efficiency across a wide pH range, Sci. Total Environ., 647 (2019) 587–596.
[22] L. Lyu, L. Zhang, C. Hu, Enhanced Fenton-like degradation of pharmaceuticals over framework copper species in copper-doped mesoporous silica microspheres, Chem. Eng. J., 274 (2015) 298–306.
[23] Y. Zhan, H. Li, Y. Chen, Copper hydroxyphosphate as catalyst for the wet hydrogen peroxide oxidation of azo dyes, J. Hazard. Mater., 180 (2010) 481–485.
[24] Y. Sun, P. Tian, D. Ding, Z. Yang, W. Wang, H. Xin, J. Xu, Y. Han, Revealing the active species of Cu-based catalysts for heterogeneous Fenton reaction, Appl. Catal., B, 258 (2019) 1–9, doi: 10.1016/j.apcatb.2019.117985.
[25] J.N. Zhu, X.Q. Zhu, F.F. Cheng, P. Li, F. Wang, Y.W. Xiao, W.W. Xiong, Preparing copper doped carbon nitride from melamine templated crystalline copper chloride for Fenton-like catalysis, Appl. Catal., B, 256 (2019) 1–12, doi: 10.1016/j.apcatb.2019.117830.
[26] M. Fang, R. Zheng, Y. Wu, D. Yue, X. Qian, Y. Zhao, Z. Bian, CuO nanosheet as a recyclable Fenton-like catalyst prepared from simulated Cu(II) waste effluents by alkaline H_2O_2 reaction, Environ. Sci.: Nano, 6 (2019) 105–114.
[27] G. Giester, E. Libowitzky, Crystal structures and Raman spectra of Cu(OH)F and $Cu_3(OH)_2F_4$, Z. Kristallogr. Cryst. Mater., 218 (2003) 351–356.
[28] L.S. Dale, An investigation of the reaction mechanism of copper fluoride carriers in the spectrochemical determination of boron and silicon, Spectrochim. Acta, Part B, 31 (1976) 515–522.
[29] Y. Zhan, X. Zhou, B. Fu, Y. Chen, Catalytic wet peroxide oxidation of azo dye (Direct Blue 15) using solvothermally synthesized copper hydroxide nitrate as catalyst, J. Hazard. Mater., 187 (2011) 348–354.
[30] H. Tian, Y. Wang, J. Zhang, Y. Ma, H. Cui, Y. Ma, Compression behavior of copper hydroxyfluoride CuOHF as a case study of the high-pressure responses of the hydrogen-bonded two-dimensional layered materials, J. Phys. Chem. C, 123 (2019) 25492–25500.
[31] E.A. Secco, G.G. Worth, Infrared spectra of unannealed and of annealed $Cu_4(OH)_6(NO_3)_2$, Can. J. Chem., 65 (1987) 2504–2508.
[32] C. Henrist, K. Traina, C. Hubert, G. Toussaint, A. Rulmont, R. Cloots, Study of the morphology of copper hydroxynitrate nanoplatelets obtained by controlled double jet precipitation and urea hydrolysis, J. Cryst. Growth, 254 (2003) 176–187.
[33] Y. Xu, D. Chen, X. Jiao, K. Xue, Nanosized Cu_2O/PEG400 composite hollow spheres with mesoporous shells, J. Phys. Chem. C, 111 (2007) 16284–16289.
[34] K. Borgohain, N. Murase, S. Mahamuni, Synthesis and properties of Cu_2O quantum particles, J. Appl. Phys., 92 (2002) 1292–1297.
[35] K. Wantala, W. Chansiriwat, R. Khunphonoi, C. Kaewbuddee, T. Suwannaruang, N. Chanlek, N. Grisdanurak, Optimization and mechanism pathways of p-cresol decomposition over Cu-Fe/NaP1 catalyst by Fenton-like process, Desal. Water Treat., 166 (2019) 122–134.
[36] T. Gu, H. Dong, T. Lu, L. Han, Y. Zhan, Fluoride ion accelerating degradation of organic pollutants by Cu(II)-catalyzed Fenton-like reaction at wide pH range, J. Hazard. Mater., 377 (2019) 365–370.
[37] T. Guo, K. Wang, G.K. Zhang, X.Y. Wu, A novel α-Fe_2O_3@g-C_3N_4 catalyst: synthesis derived from Fe-based MOF and its superior photo-Fenton performance, Appl. Surf. Sci., 469 (2019) 331–339.

[38] H. Fida, G.K. Zhang, S. Guo, A. Naeem, Heterogeneous Fenton degradation of organic dyes in batch and fixed bed using La-Fe montmorillonite as catalyst, J. Colloid Interface Sci., 490 (2017) 859–868.
[39] Z. Ai, Y. Wang, M. Xiao, L. Zhang, Microwave-induced catalytic oxidation of RhB by a nanocomposite of Fe@Fe_2O_3 core-shell nanowires and carbon nanotubes, J. Phys. Chem. C, 112 (2008) 9847–9853.
[40] Z. He, C. Sun, S. Yang, Y. Ding, H. He, Z. Wang, Photocatalytic degradation of rhodamine B by Bi_2WO_6 with electron accepting agent under microwave irradiation: mechanism and pathway, J. Hazard. Mater., 162 (2009) 1477–1486.
[41] C.C. Kuan, S.Y. Chang, S.L.M. Schroeder, Fenton-like oxidation of 4-chlorophenol: homogeneous or heterogeneous?, Ind. Eng. Chem. Res., 54 (2015) 8122–8129.

Supplementary information

Solvothermal synthesis of spherical copper hydroxyfluoride (CuOHF) and its heterogeneous Fenton catalytic activity

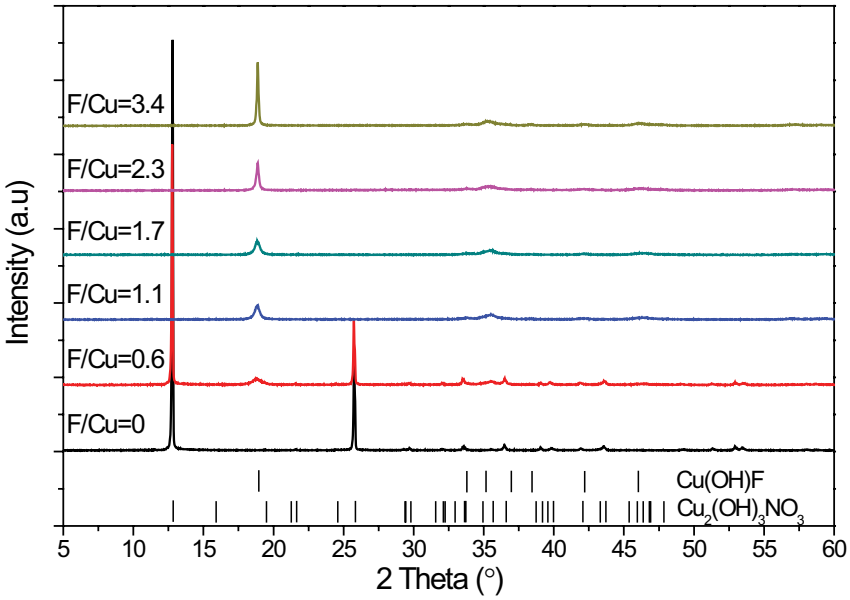

Fig. S1. XRD patterns of the products synthesized under various amount of HF.

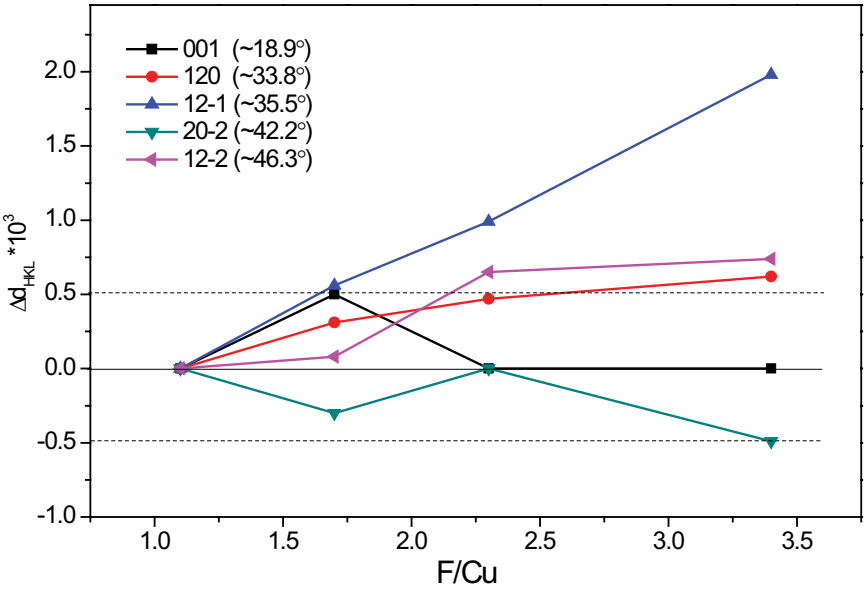

Fig. S2. Interplanar spacing changes of the synthesized CuOHF with F/Cu ratio (based on the F/Cu = 1.1).

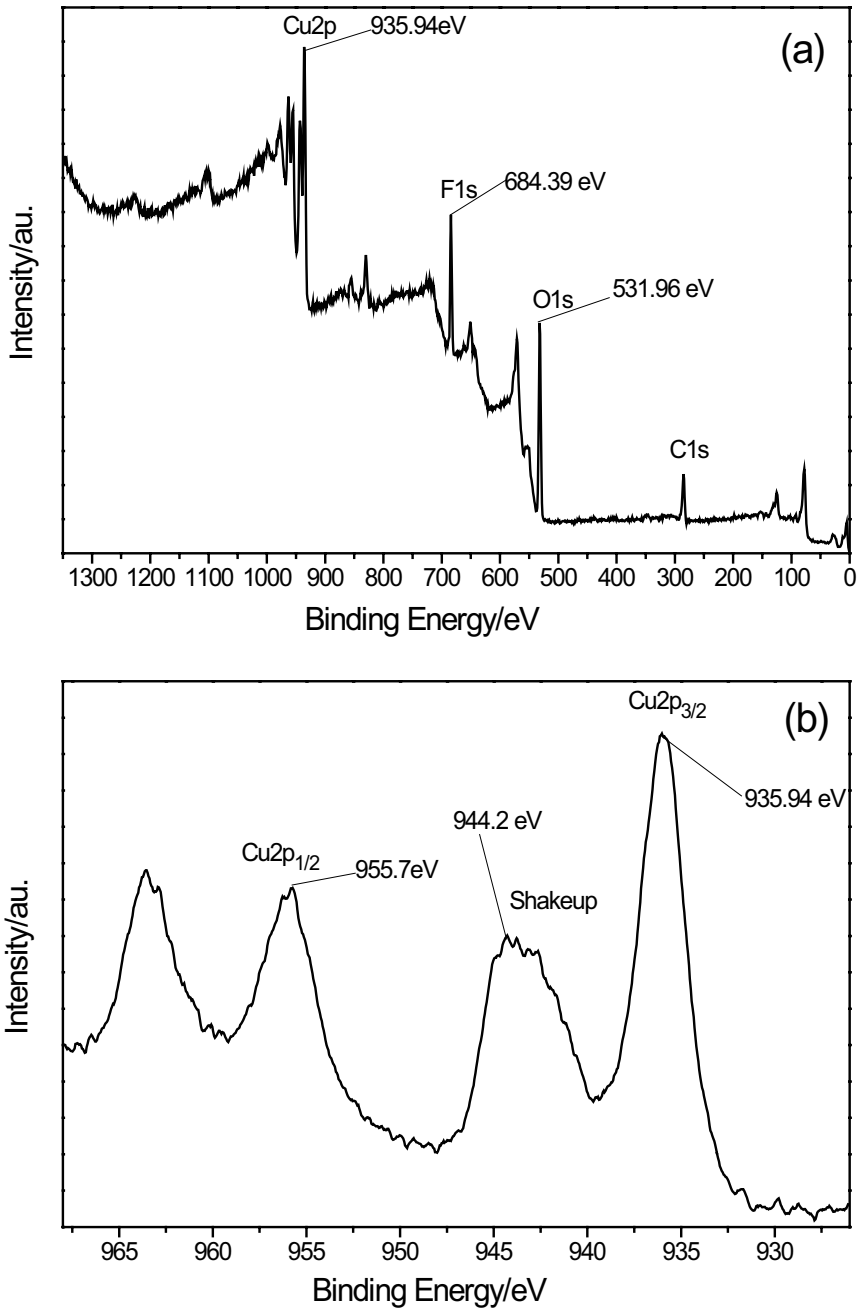

Fig. S3. XPS (a) survey scan and (b) high-resolution spectrum of Cu_{2p} of the spherical CuOHF.

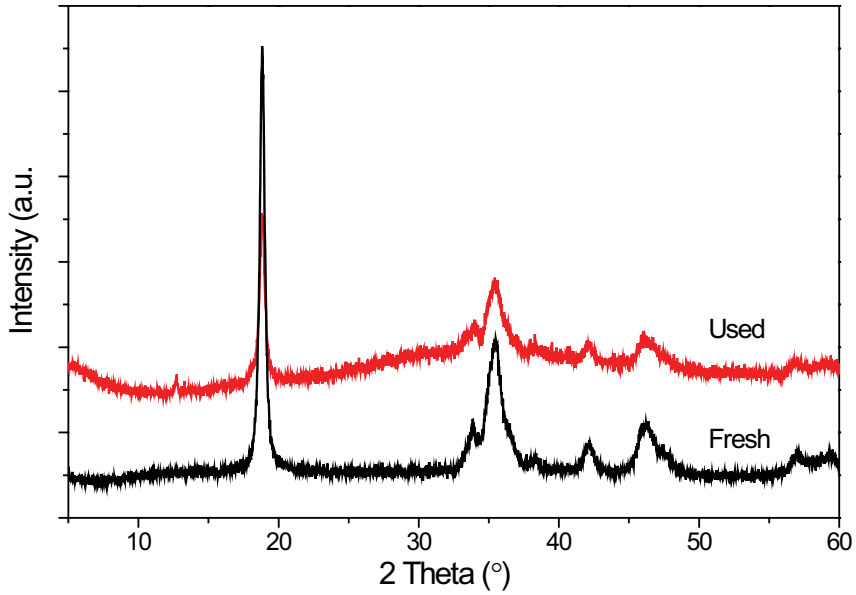

Fig. S4. XRD patterns of the spherical CuOHF before and after use.

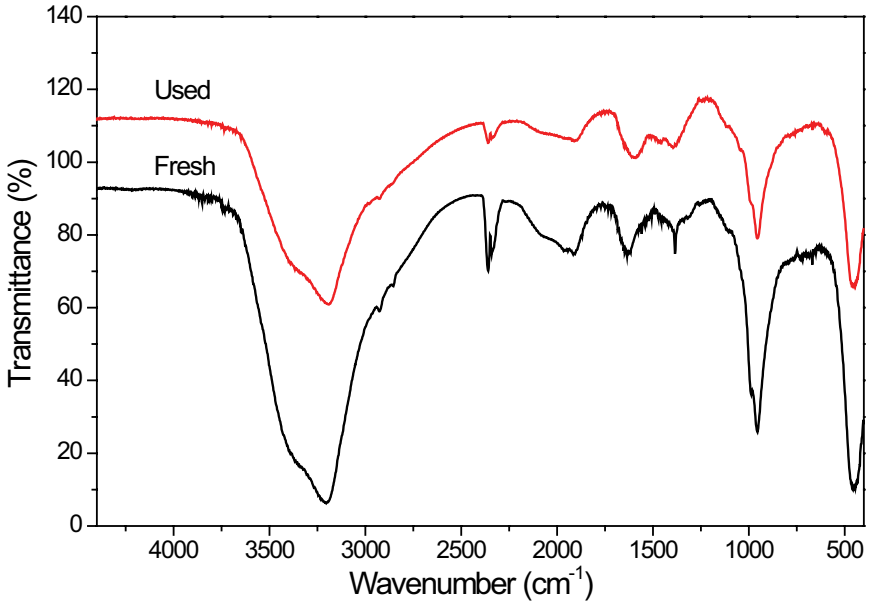

Fig. S5. FTIR spectra of the spherical CuOHF before and after use.

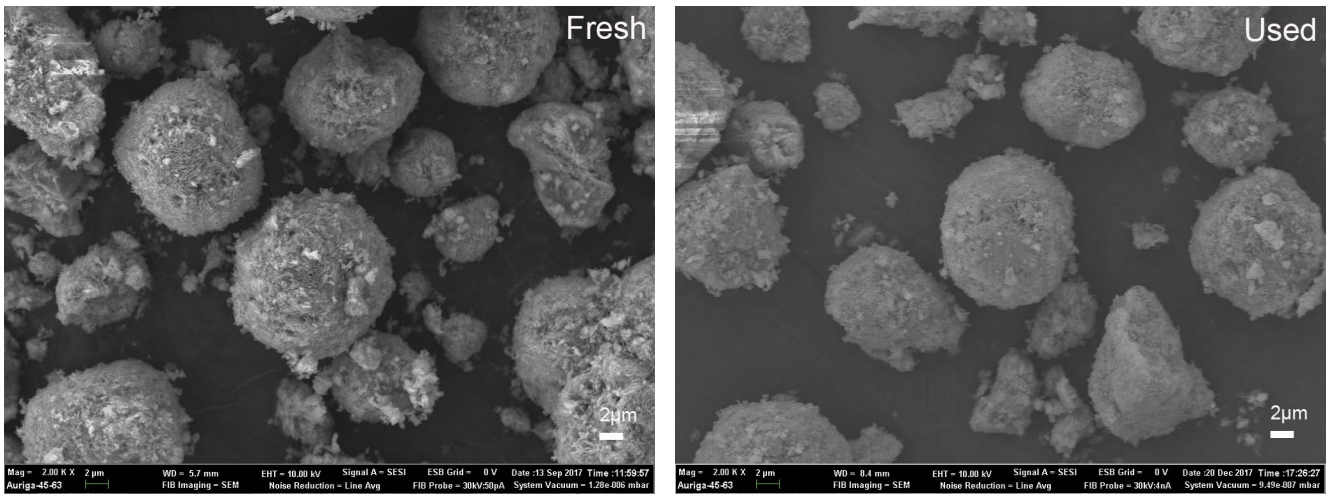

Fig. S6. SEM images of the spherical CuOHF before and after use.